

Analysis and chemical composition of larnite-rich ultrarefractory materials

J. Martínez-Frías^{a,*}, R. Benito^b, G. Wilson^c,
A. Delgado^d, T. Boyd^e, K. Marti^f

^a Centro de Astrobiología (CSIC/INTA), Instituto Nacional de Técnica Aeroespacial, Ctra de Ajalvir, km 4, 28850 Torrejón de Ardoz, Spain

^b Departamento de Geología, Museo Nacional de Ciencias Naturales, CSIC, Madrid, Spain

^c ISOTRACE Laboratory, University of Toronto, 60 St. George Street, Toronto, Ont., Canada M5S 1A7

^d Laboratorio de Isótopos Estables, Estación Experimental del Zaidín, CSIC, Profesor Albareda 1, 18008 Granada, Spain

^e Department of Geology, University of Toronto, Toronto, Ont., Canada M5S 3B1

^f Department of Chemistry, University of California, San Diego, 9500 Gilman Drive, La Jolla, CA 92093, USA

Accepted 27 November 2003

Abstract

Larnite (β - Ca_2SiO_4) is a rare, little known compound. However, despite its scarcity, larnite is found in different natural settings, almost always under thermodynamic conditions of around 0.2–1 kbar and 1000–1100 °C. Larnite can also be formed artificially, especially during the synthesis of high technology refractory and ceramic materials, and as a mineral component of some industrial slags and portland cements. This work describes the analysis and compositional properties of larnite-rich ultrarefractory materials, cataloged as possible meteorite specimens, from the collection of the “Museo Nacional de Ciencias Naturales” (Madrid). Larnite is associated with metal oxides and sulfides, native iron and copper, and calcium-aluminium silicates. Bulk chemical composition was determined by XRF (specific standards and analytical routines were designed). Minor and trace elements (including rare earths) were analyzed by the combination of INAA, ICP-MS and ICP-AES. Larnite occurs as imperfectly developed tabular crystals, mainly displaying rhombic shapes of around 25 mm \times 35 mm. SEM and microprobe analyses indicate its chemical composition closely matches the theoretical formula ($x = \text{Ca}_{1.96}\text{Si}_{0.98}\text{O}_4$), although significant amounts of Al ($\text{Al}_{0.19}\text{--}\text{Al}_{0.54}$), Fe ($\text{Fe}_{0.01}\text{--}\text{Fe}_{0.14}$), Mn ($\text{Mn}_{0.01}\text{--}\text{Mn}_{0.03}$) and Mg ($\text{Mg}_{0.01}\text{--}\text{Mg}_{0.02}$) have also been detected in some crystals. PIXE analyses display high Fe and Ba values, ranging from 3.9 to 8.4 wt.%, and from 1058 to 1530 ppm, respectively.

© 2004 Elsevier B.V. All rights reserved.

Keywords: Larnite; X-ray fluorescence; Standards; Chemical composition; Meteorite

1. Introduction

Larnite (β - Ca_2SiO_4) forms part—along with forsterite (Mg_2SiO_4), fayalite (Fe_2SiO_4), and tephroite (Mn_2SiO_4)—of the monticellite and knebelite series (general group of olivine). It has been found in different geological settings, almost always under thermodynamic conditions [1] of around 0.2–1 kbar and 1000–1100 °C. These settings include kimberlitic magmas, carbonatites, skarns and ore mineral deposits. Thus, larnite occurs, among others, in: (a) the Oldoinyo Lengai volcano (Tanzania) associated with wollastonite, combeite and melilite [2]; (b) nephelinites and basanites from the Freemans Cove area, Bathurst island,

Canadian Arctic Archipelago [3]; (c) Houghton impact crater, Canada, where high-temperature interactions have occurred between molten silicates and carbonates [4]; (d) Carneal and Scawt Hill areas (Ireland) as mineral associations developed by metamorphic and metasomatic reactions [5]; (e) in the Hatrurim Formation (Israel) [6]; (f) the ore deposit of Koktenkol, central Kazakhstan [7]; (g) in the ultramafic alkaline Gardiner Complex (East Greenland) [8], and (h) as small grains (3 mm) associated with wollastonite and andradite in dark inclusions in the Bali (CV3) carbonaceous chondrite [9]. Very recently, it has been proposed that larnite could have formed in the vapor plume following the Cretaceous-Tertiary (K-T) impact and have neutralized enough acid to make water safe for freshwater species within hours of the blast [10]. Larnite can also be produced artificially, especially during the synthesis of high technology refractory and ceramics materials, and as

* Corresponding author. Tel.: +34-91-5206418; fax: +34-91-5201621.
E-mail address: martinezfrias@mncn.csic.es (J. Martínez-Frías).

a mineral component of some industrial slags and Portland cements [11].

This work describes the in-depth study of the first occurrence of unusual larnite-rich rocks from Spain (Fig. 1). These rocks come from the mineral collection of the “Museo Nacional de Ciencias Naturales” in Madrid. Besides the interest of the singularity of their mineral paragenesis, these larnite-rich rocks are of utmost importance and are labeled, “rocks of possible meteoritical origin”, in relation with the well documented 1994 impact in the area of Getafe (a town south of Madrid) [12–14]. These materials exhibit a complex assemblage involving native, oxide and silicate minerals (mainly native iron, wustite, larnite).

The study of this unusual larnite-rich ultrarefractory material provides: (a) a detailed account of the sample fusion, calibration, instrumentation methods for the analysis of whole-rock major elements by X-ray fluorescence (XRF). XRF specific standards and analytical routines were designed. Several aspects of sample preparation and instrument performance which are important considerations for accurate analysis are also discussed; (b) the chemical results obtained from this analysis, (c) whole-rock determinations of minor and trace elements (including rare earths) by the combination of INAA, ICP-MS and ICP-AES) further chemical information regarding the concentration values of trace elements in larnite and their principal associated mineral phases.

2. Compositional characteristics

The larnite-rich materials consist of metallic inclusions of native iron embedded in a very fine grain matrix rich in silicates (mainly larnite and melilite, of gehlenite type) and oxides (mainly wustite and small amounts of chromite) (Fig. 2A–F).

Minor grains displaying spinel- and perovskite-type compositions (closely associated with melilite as a dark, apparently glassy groundmass), and minute grains of troilite, corundum, and native copper were also detected within the matrix. Although it is difficult to establish a clear crystallization sequence, ore textures seem to reflect a combination of several processes including: rapid cooling and rapid growth (quenching) from a liquid (proved by the presence of acicular, dendritic and spherulitic textures), varying proportions of melted and crystallized zones and, probably recrystallization.

Larnite and wustite, are the main components of the matrix. Larnite occurs as imperfectly developed mainly rhombic tabular crystals (Fig. 2C) of around $25\ \mu\text{m} \times 35\ \text{mm}$. Holes and small cracks are common within some crystals. Apart from the individual textural characteristics of the different mineral phases described further, the most peculiar texture of the larnite-rich materials involves chromite (or chromite-melilite) cores and flower-type wustite rims (Fig. 2F).

2.1. X-ray fluorescence analysis

X-ray fluorescence analysis of fused glass discs is among the most common methods for determining the major- and minor-element compositions of silicate, carbonate and oxide materials. There are many natural standards, with high silicon, calcium and iron contents, which can be used for establishing the calibration curves as a function of the compositional characteristics of the samples. Nevertheless, due to the relative amounts of these elements in the larnite-rich ultrarefractory material, the use of specific standards and their mixture was necessary to obtain a matrix compositionally similar to the problem samples. A classic procedure involves mixing pure chemical compounds; this requires either the previous weighing of very low quantities of some of these compounds, or the preparation of a high quantity of each standard. There is a problem with this second procedure related to the representative homogenization of the sample before the preparation of the fused glass discs. In this work, we have obtained new calibration standards combining pre-existing standards at different relative proportions. The main advantages of this procedure are that a previous homogenization is not necessary as it occurs during fusion and less number of weighing is required.

The preparation procedures of glass discs work well for many materials. The samples were ground to <200 mesh, dried at $110\ ^\circ\text{C}$. A $0.30 \pm 0.02\ \text{g}$ aliquant is weighed accurately and mixed with 5.50 g of spectroscopic grade lithium tetraborate flux ($\text{Li}_2\text{B}_4\text{O}_7$), which has been previously dried at $400\ ^\circ\text{C}$ for 6 h. 0.10 g of LiBr is added as a non-wetting agent. The mixture is then fused in a covered Pt (95%)–Au (5%) crucible for 10 min [15]. The fusion is performed within a Philips-Soled PERL’X2 automatic bead machine. During the fusion, the crucible is rotated off-axis to ensure mixing of the melt. The molten mixture is then poured into a Pt (87%)–Au(10%)–Rh(3%) mold which is heated red-hot, and allowed to solidify without quenching.

A preliminary analysis was made using the classic calibration routine for silicate rocks to determine the concentration ranges of the larnite-rich materials. These routines use natural standards (granite, basalt, andesite, soils and sediments). The first results (in wt% oxides) were CaO: 33, Fe_2O_3 : 26, SiO_2 : 16, Al_2O_3 : 11, MnO: 5 and MgO: 4. P_2O_5 , TiO_2 and K_2O were below 1%. Subsequently, specific standards were prepared covering the following concentration ranges: CaO: 20–40%, Fe_2O_3 : 20–35, SiO_2 : 10–20 and Al_2O_3 : 5–15.

Standards directly used were artificial basic slags (BCS381, BCS382, BCS382/1 and BCS174/2), and a natural silicate-rich rock (NBS-688). NBS-688 is a finely powdered basalt rock that was obtained from a Cenozoic basalt flow near Jackpot, NV (USA). In addition, BCS382, BCS382/1 and BCS174/2 standards were mixed with FER1, FER2 and FER4. The mixing ratio BCS:FER was 2:1. FER1 was obtained from a bed of magnetite-quartz iron-formation at Austin Brook near Bathurst, New Brunswick. These minerals comprise 55 and 30%, respectively, of the volume of the

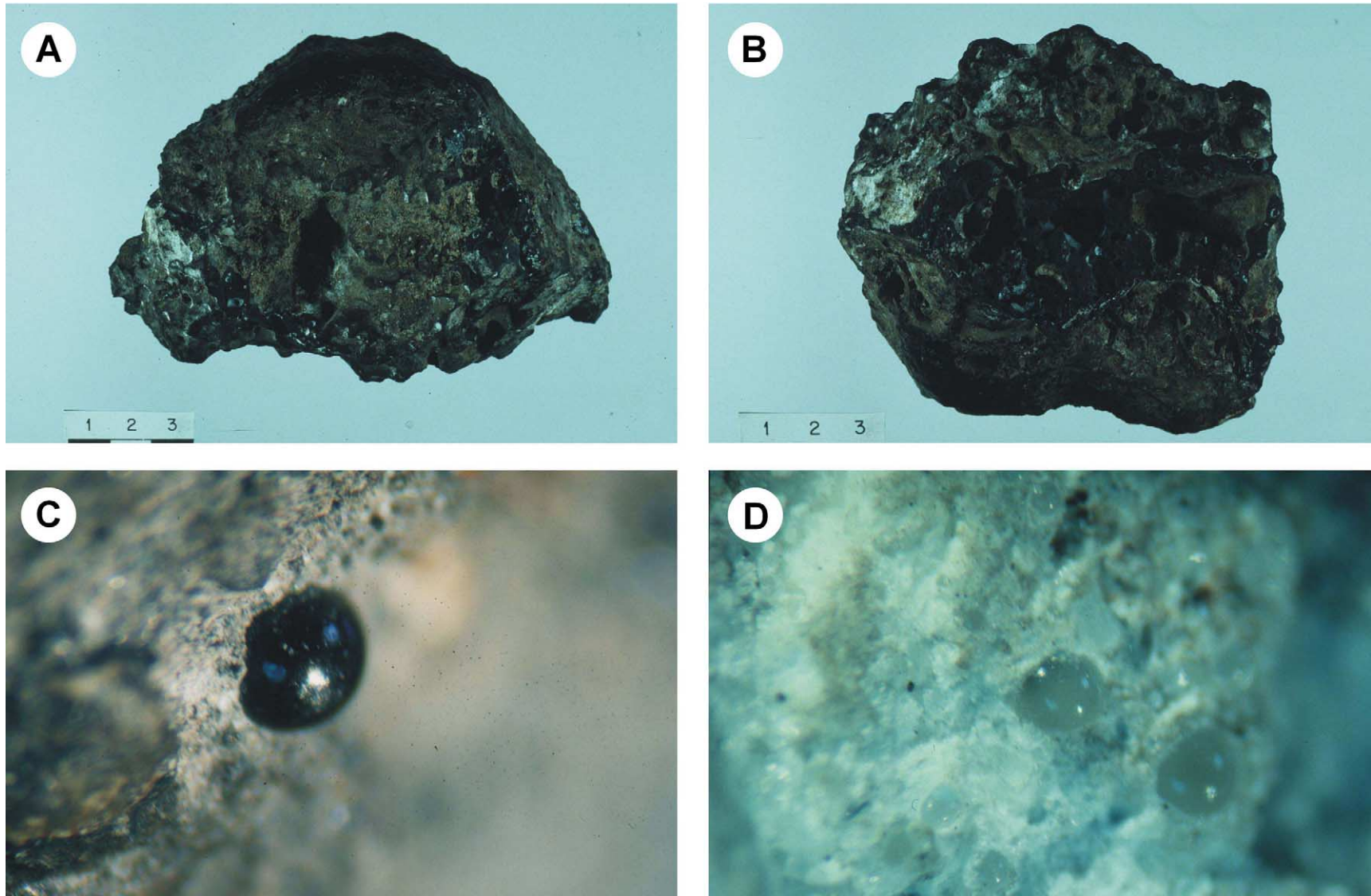


Fig. 1. Typical specimen of larnite-rich rocks. Note its semi-oriented shape displaying smooth (A) and rough surfaces (B) and its scoriaceous texture. Color and textural differences exist between surface (melting patina) and interior. Black (C) and milky (D) glassy droplet-globules are found scattered on the surface of this ultrarefractory material.

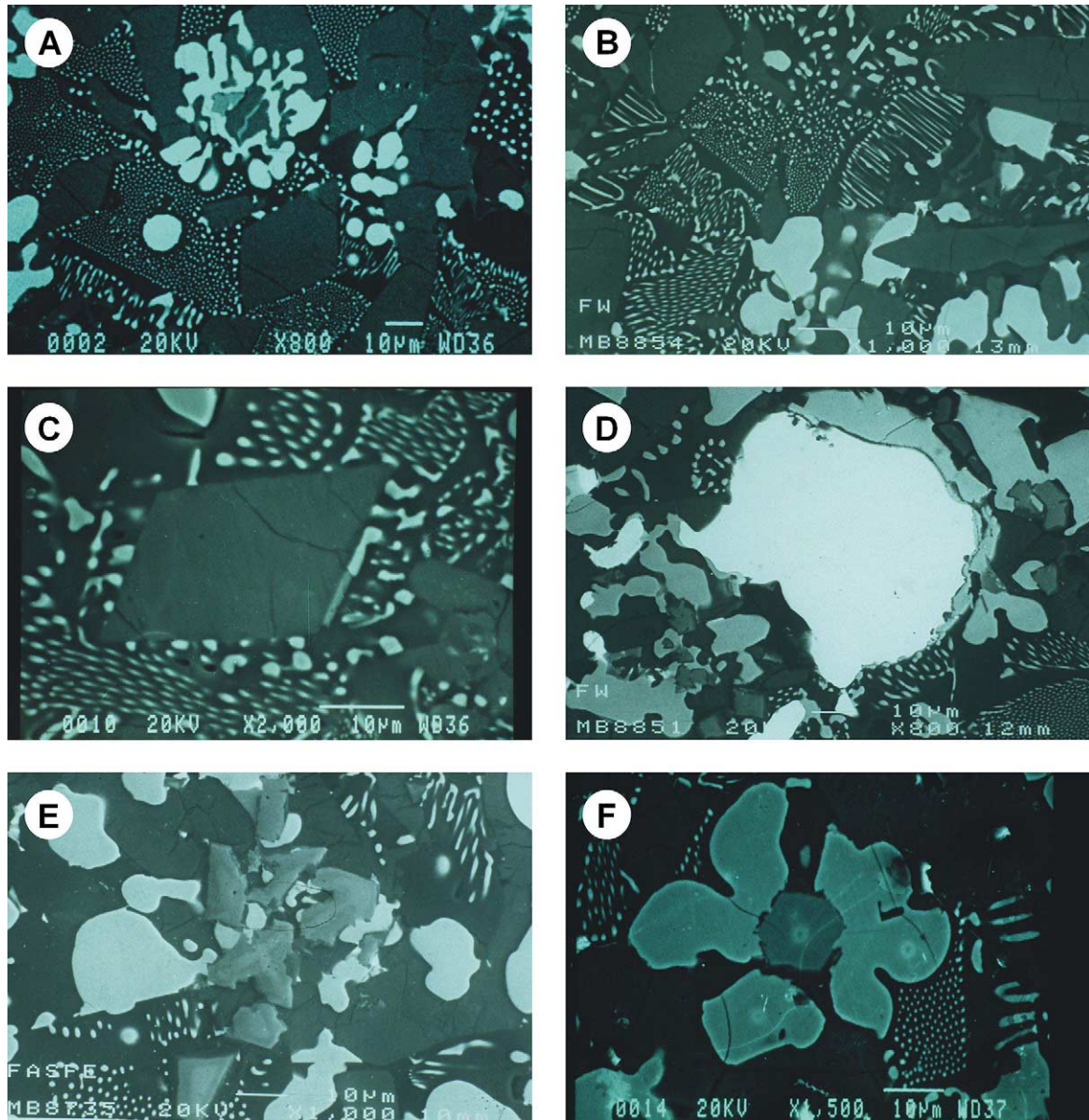


Fig. 2. SEM pictures representing the paragenetic associations of the larnite-rich materials and displaying the main mineral phases and textural relations. (A) Rhombic crystals of larnite associated to wustite (white globular and irregular grains) and chromite (light gray) in the dark, apparently glassy groundmass of melilite (gehlenite type). (B) Irregular grains and unmixing blebs, rods and lamellae of wustite associated with the euhedral grains of larnite. (C) Euhedral crystal of larnite. Note the presence of intracrystalline small fractures and cracks. (D) Irregular grain of native iron partially rimmed by wustite. (E) Skeletal crystal of chromite displaying an apparent preferential growth towards the apices (cruciform type). (F) The most peculiar texture of these larnite-rich materials involves chromite (or chromite-melilite) cores and flower-type wustite rims.

sample. The hematite content is about 3%. FER2 is from an iron-formation bed occurring in greywacke in the north pit of the Griffith Mine at Bruce Lake, Ontario. Magnetite forms about 25% of the sample by volume. Amphibole and quartz are the major gangue constituents. FER4 is from the Sherman Mine property at Temagami, Ontario. This standard was taken in the south pit from a cherty magnetite iron-formation containing chloritic tuff. Quartz is the most abundant mineral present. Hematite occurs as dusty inclusions in the quartz, but as micro-laminae in jasper layers.

Table 1 displays the bulk chemical composition of the standards and mixtures. Major elements are measured with a Philips PW-1404 sequential spectrometer with a Sc/Mo source tube, using the counting conditions listed in Table 2.

Four analyzing crystals were used for the detection of the K_{α} intensities: LIF (200) for Ti, Fe, Mn, Ca and K, PET for Si and Al, PX1 for Mg and Ge for P. In the calibration procedure, the samples are weighed according to both compositional uncertainties and counting statistical errors, using York's (1966) linear least-squares fitting procedure. The calibration data presented in this paper were obtained

Table 1
Bulk chemical composition of the artificial and natural standards and mixtures

	BCS381	BCS174/2	BCS382/1	BCS174/2 + FER1	BCS382 + FER1	BCS382	BCS382/1 + FER4	BCS382 + FER2	NBS688
SiO ₂	8.78	11.20	13.03	13.20	18.65	19.50	25.38	29.40	48.35
Al ₂ O ₃	0.67	0.77	3.79	0.69	5.18	7.51	3.09	6.73	17.35
Fe ₂ O _{3(T)}	19.02	22.73	28.45	40.44	34.40	13.67	32.27	22.18	10.34
MnO	3.16	3.80	7.96	2.61	6.21	9.20	5.37	6.17	0.17
MgO	1.03	4.63	3.73	3.19	7.23	10.70	2.96	7.83	8.46
CaO	49.00	43.20	40.10	29.90	23.10	33.00	27.48	22.72	12.17

Table 2
Counting conditions for the main major elements

Element	Collimator	Crystal	2θ	LL	UL
Si	Fine	PE	109.165	35	85
Al	Coarse	PE	145.035	34	82
Fe	Fine	LiF200	57.535	42	72
Mn	Fine	LiF200	62.980	45	75
Mg	Coarse	PX1	22.880	30	85
Ca	Fine	LiF200	113.155	35	75

Sc/Mo target, 40 kV, 70 mA. K α lines first order. Flow proportional counter with 90% Ar, 10% CH₄, vacuum path. Filter out. Samples rotated. LL: lower level, UL: upper level.

using nine reference materials. Fig. 3 shows typical calibration curves for Ca, Fe and Si, respectively.

The exact chemical analysis of the larnite-rich materials is (in wt% oxides) CaO: 34.78, Fe₂O₃: 26.55, SiO₂: 16.27, Al₂O₃: 10.73, MnO: 5.69, MgO: 3.37, P₂O₅: 0.61, TiO₂: 0.57 and K₂O: 0.02. As previously defined, chromite occurs as an accessory mineral by which an additional calibration for Cr was also carried out giving a result of 1.42 wt.% Cr₂O₃. This completes an extremely accurate total analysis of 100.01.

3. Trace elements and chemistry of minerals

Trace elements (including REE) were determined by a combination of INAA, ICP-MS, ICP-AES and AAS. Small quantities of base metals were detected: Zn: 332 ppm, Cu: 170 ppm, Sn: 40 ppm and Pb: 12 pp. The refractory elements Zr, Nb, Sr and Ba are extremely high (168, 66, 174 and 2118 ppm, respectively) and Y and V are 6 and 400 ppm; Sc is low: <1 ppm, and the light REE (La, Ce) are 10 and 118 ppm. The heavy REE are, in broad terms, less enriched. The Ni content is 18 ppm.

The chemical characteristics of larnite and its associated minerals were studied using scanning electron microscopy (SEM) and electron microprobe. For SEM studies the specimens were coated with gold (20 nm) in a Bio-Rad SC515 sputter coating unit. General SEM observations were made in a Philips XL20 SEM at accelerating voltages of 20–30 kV. Energy-dispersive X-ray microanalyses (EDX) were obtained using a Phillips EDAX PV9900 with a light element detector type ECON. The crystal-chemical

characteristics of the minerals were determined on the basis of a large data series of electron microprobe analyses (Jeol Superprobe JXA-8900M), bulk and channel-selected (TAP, PETJ, LIF, PETH) X-ray spectra search and identification routines. Natural standards and synthetic crystals from the collection of the “Servicio de Microscopía Electrónica Lluís Bru”, Complutense University, Madrid were used.

Microprobe analyses of larnite euhedral crystals and anhedral mineral grains indicate they closely match the theoretical formula ($x = \text{Ca}_{1.96}\text{Si}_{0.98}\text{O}_4$), although significant amounts of Al (Al_{0.19}–Al_{0.54}), Fe (Fe_{0.01}–Fe_{0.14}), Mn (Mn_{0.01}–Mn_{0.03}) and Mg (Mg_{0.01}–Mg_{0.02}) have been detected in some crystals. These elements broadly conform to the following average general formula: Ca_{1.60}Al_{0.34}Fe_{0.09}Mn_{0.03}Mg_{0.01}Si_{0.90}O₄.

The microprobe analyses of the other major and minor minerals occurring in the larnite-rich materials show native iron displaying a relatively pure composition. Some minor (Mn, Mg, Ca) and trace (Cl, Cr, Si) elements were found, up to around 6 wt.%. The average composition is: FeO: 92.15, MnO: 4.57, MgO: 1.78, CaO: 0.97. Wustite contains small amounts of Mn, Mg and Ca. The average formula is Fe_{0.77}Mn_{0.15}Mg_{0.11}Ca_{0.02}O, with values of almost pure Fe (Fe_{0.92}). Melilite does not closely match the theoretical formula. Small amounts of Ti, Fe, Mn and Mg are always present. Erratic traces of Ir (around 0.10 wt.%) were also detected in some grains. The average formula is Ca_{1.98}Al_{2.00}Fe_{0.20}Mn_{0.03}Si_{0.86}O₇. Chromite displays variable composition. The average formula is Cr (Cr_{0.99}–Cr_{1.54}), Al (Al_{0.33}–Al_{0.75}), Fe (Fe_{0.33}–Fe_{0.48}) and Mg (Mg_{0.35}–Mg_{0.47}). Spinel and perovskite occur associated as mixed mineral grains. However, whereas perovskite matches the theoretical formula (CaTiO₃: Ca_{1.10}Ti_{0.72}Al_{0.14}Fe_{0.12}Si_{0.03}Cr_{0.03}O₃ (although there are substitutions of Al by Ti: Ca_{1.08}Al_{1.12}Si_{0.08}Fe_{0.03}O₃), spinel displays compositional variations. In general terms, it matches the average formula: Al_{1.76}Mg_{0.50}Fe_{0.45}Ca_{0.10}Mn_{0.14}Si_{0.04}Cr_{0.02}O₄. As previously defined, minute grains of corundum, native copper and troilite were also detected within the matrix of the larnite-rich materials. Corundum contains small amounts of Fe (Al_{1.91}Fe_{0.07}O₃). Both native copper and troilite display very pure compositions.

Specific Proton Induced X-ray Emission (PIXE) probe analyses were also carried out on 18 selected mineral targets (3 larnites, 6 on native iron, 2 metal–oxide (wustite)

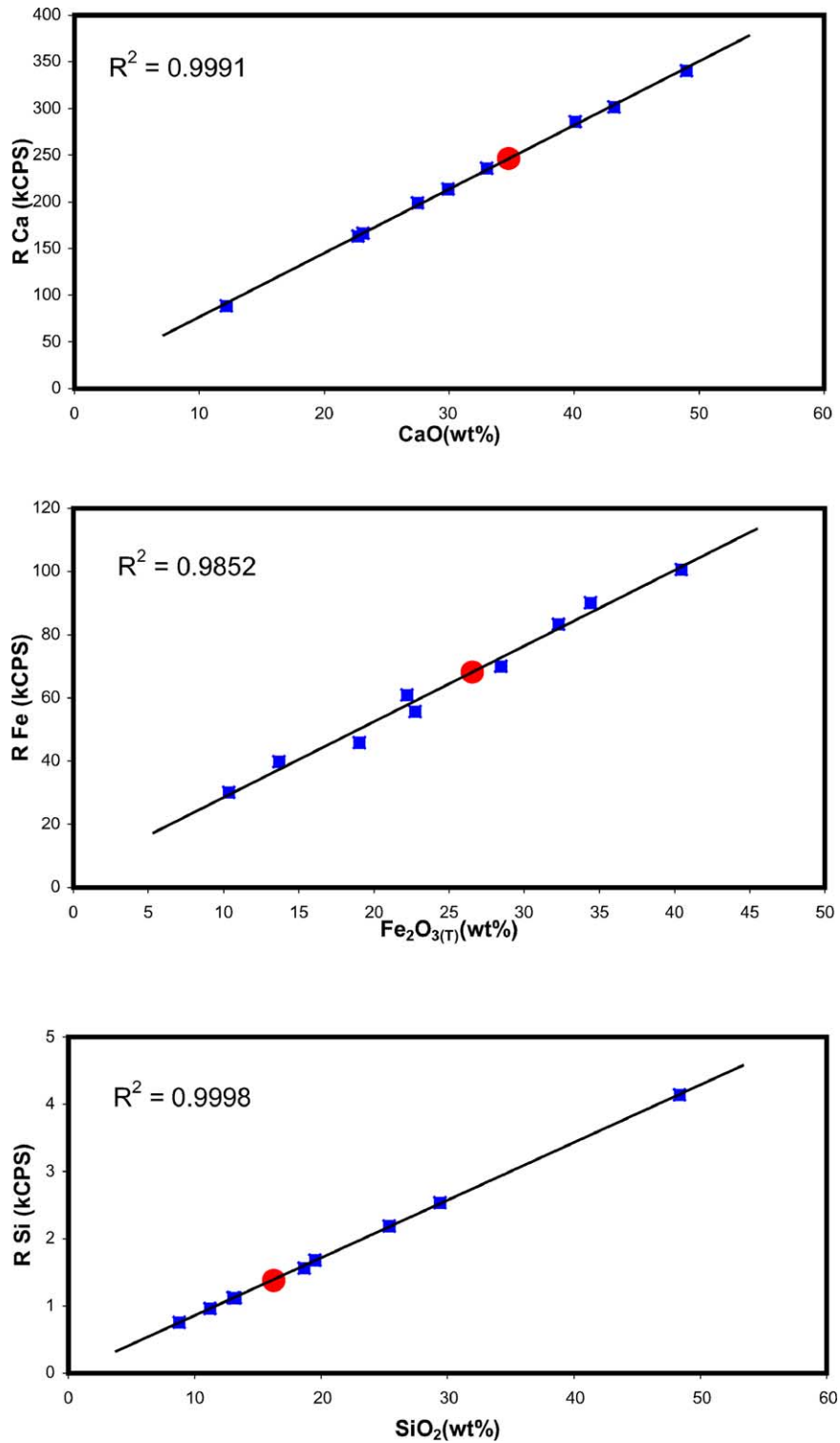


Fig. 3. Calibration curves for Ca, Fe and Si. Intensity vs. concentration. Squares: standards (see Table 1); circle: larnite-rich ultrarefractory material.

blebs and 7 melilites). The PIXE data presented for 16 elements add a further dimension to the electron probe analyses. The first general findings do not concern the presence of elements, but instead, the absence of certain groups which were specifically expected for their chemical affinity. Elements, such as the platinum group elements (PGE) and the

rare earths (REE), are not present at a level significantly above the quoted minimum detection limits. A more sensitive method, such as the ion microprobe (SIMS) would have been required to detect PGE in metals or REE in melilites. Generalized minimum detection limits for elements are as follows: In metal; Ru, Rh, Pd and Ag (7 ppm), Re, Os, Ir, Pt

and Au (20–40 ppm, declining from Re to Au), Ge and Se (10 ppm), Te (15 ppm) and Hg, Tl, Pb and Bi (20–30 ppm). In silicates; Rb (3 ppm), Te (25 ppm), Cs (50 ppm), La (30 ppm in larnite, 80 ppm in melilite), U and Th (8 ppm).

PIXE analyses of three single larnite crystals displayed high Fe and Ba values ranging from 3.9 to 8.4 wt.%, and from 1058 to 1530 ppm, respectively. Native iron shows significant amounts of Cu (17,590 ppm) and traces of Co, Ni, Mo, Sn and W ranging from 200 to 300 ppm. The Ni content is <0.03%. Wustite also presents high contents of Cu (2050 ppm). Finally, the analyses of melilite indicates it is alkali-enriched, with $\geq 0.1\%$ combined Sr and Ba, at an average Ba/Sr ratio ≥ 4 . Traces of Y and Zr are present, and $\geq 15\%$ Fe. Melilite contains appreciable Zn (130 ppm higher than iron).

4. Conclusion

This study has established the exact chemical characterisation of larnite (b-Ca₂SiO₄) rich ultrarefractory materials in Spain. XRF analysis has revealed to be a highly effective geochemical technique for the determination of major elements. However, due to the unusual composition of the specimens, the preparation of new standards was necessary to obtain a matrix compositionally similar to the problem samples. The new calibration curves have allowed accurate values for all elements to be obtained (in particular for calcium, displaying a chemical difference of up to 2 wt% CAO in relation to the classic calibration of silicates). The analysis of minor and trace elements, by a combination of INAA, ICP-AES and ICP-MS, reflects: (a) a high content of some refractory elements (Zr: 168 ppm, Nb: 66 ppm, Sr: 174 ppm and Ba: 2118 ppm) and (b) small quantities of base metals: Zn: 332 ppm, Cu: 170 ppm, Sn: 40 ppm and Pb: 12 ppm. Finally, the combination of electron microprobe and PIXE analyses have identified two compositional types of larnite crystals in accordance with their textural differences. Thus, euhedral rhombic-shape larnite crystals display compositions which closely match the theoretical formula, whereas the anhedral larnite grains contain impurities of Al, Fe, Mn and Mg.

Acknowledgements

This study was carried out with the financial support of the Spanish “Comisión Interministerial de Ciencia y Tecnología (CICYT) and “Consejo Superior de Investigaciones Científicas (CSIC) and forms part of the research project regarding meteorites of the Centro de Astrobiología (CSIC-INTA, associated to the NASA Astrobiology Institute). Thanks to J.M. Martín, R. González, M^a I. Ruiz, M. Vallejo, J. Arroyo and R. Sanchez (MNCN, CSIC), J.A. Rodríguez-Losada (ULL), J. Antonio Martín-Rubi, S. del Barrio, J. Menduñía and M. Fernández (IGME), J. Ruck-

ledge (ISOTRACE), J. Izquierdo and F. Montero (IBERDROLA), A. Formoso, A. Gomez-Coedo and M^a T. Dorado (CNIM, CSIC), J.M^a. Fernández-Navarro (ICV, CSIC), and A. Rodríguez-Muñoz and J.L. Baldonado (UCM). Special thanks to Paul Gibling.

References

- [1] I.V. Veksler, T.F.D. Fedorchuk, Nielsen Phase equilibria in the silica-undersaturated part of the KAlSiO₄–Mg₂SiO₄–Ca₂SiO₄–SiO₂–F system at 1 atm and the larnite-normative trend of melt evolution, *Contrib. Miner. Petrol* 131 (1998) 347–363.
- [2] J.B. Dawson, J. Keller, C. Nyamweru, Historic and recent eruptive activity of Oldoinyo Lengai, in: K. Bell, J. Keller (Eds.), *Carbonatite Magmatism: Oldoinyo Lengai and the Petrogenesis of Natrocarbonatites*, Springer-Verlag, Berlin Heidelberg, 1995, p. 210.
- [3] R.H. Mitchell, R.G. Platt, The Freemans Cove volcanic suite; field relations, petrochemistry, and tectonic setting of nephelinite-basanite volcanism associated with rifting in the Canadian Arctic Archipelago Can, *J. Earth Sci.* 21 (4) (1984) 428–436.
- [4] I. Martínez, P. Agrinier, U. Schaerer, M. Javoy, A SEM-TEM and stable isotope study of carbonates from the Haughton impact structure, *Canada Earth Planet. Sci. Lett.* 121 (3–4) (1994) 559–574.
- [5] P.A. Sabine, M.T.T. Styles, B.R. Young, Gehlenite, an exomorphic mineral from Carneal, Co. Antrim, Northern Ireland, *Miner. Mag.* 49 (354) (1985) 663–670.
- [6] S. Gross, The mineralogy of the Hatrurim Formation, Israel. *GSI bull.* 70, 1977.
- [7] L.D. Krigman, I.V. Veksler, R.A. Ishbulatov, T.F.D. Nielsen, Phase equilibria in the silica-undersaturated part of the normative kalsilite-forsterite-larnite-quartz-H₂O tetrahedron at 0.2 Gpa, in: *Proceedings of the EUG XI, Strasbourg, France, 8–12 April, European Union of Geosciences, J. Conf. (Abstracts)* 6 (2001) 578.
- [8] T.F.D. Nielsen, I.P. Solovova, I.V. Veksler, Parental melts of melilitite and origin of alkaline carbonatite: Evidence from crystallized melt inclusions, Gardiner complex, *Contrib. Miner. Petrol* 126–124 (1997) 331–344.
- [9] M.A. Nazarov, G. Kurat, F. Brandstätter, Silica-bearing objects in Bali (CV3): a novel type of inclusion in carbonaceous chondrites, in: *Proceedings of the 61st Annual Meteoritical Society Meeting (Abstract 5123, pdf)*.
- [10] T. Maruoka, Ch. Koeberl, Acid-neutralizing scenario after the Cretaceous-Tertiary impact event, *Geology* 31-6 (2003) 489–492.
- [11] M. Castellote, C. Andrade, C. Alonso, X. Turrillas, Å. Kvik, A. Terry, G. Vaughan, J. Campo, Synchrotron radiation diffraction study of the microstructure changes in cement paste due to accelerated leaching by application of electrical fields, *J. Am. Ceram. Soc.* 85-3 (2002) 631–635.
- [12] J. Martínez-Frías, La caída de la roca de supuesto origen meteorítico de Getafe, *Dept. Com. y Prensa CSIC* (1994) 1–3.
- [13] J. Martínez-Frías, La roca de Getafe: trayectoria de caída efectos del impacto y marcadores morfotexturales de vuelo, *Geogaceta* 25 (1998) 215–218.
- [14] J. Martínez-Frías, A. Weigel, K. Marti, T. Boyd, G.H. Wilson, T. Jull, The Getafe rock: fall, composition and cosmic ray records of an unusual ultrarefractory scoriaceous material, *Revista de Metalurgia* 35 (1999) 308–315.
- [15] R.A. Couture, M.S. Smith, R.F. Dymek, X-ray fluorescence analysis of silicate rocks using fused glass discs and a side-window Rh source tube: accuracy precision and reproducibility, *Chem. Geol.* 110 (1993) 315–328.